Data in Brief 10 (2017) 576–582

Contents lists available at ScienceDirect

Data in Brief

journal homepage: www.elsevier.com/locate/dib

Data Article

Dataset on the structure and thermodynamic and dynamic stability of Mo_2ScAlC_2 from experiments and first-principles calculations

Martin Dahlqvist*, Rahele Meshkian, Johanna Rosen

Department of Physics, Chemistry and Biology (IFM), Linköping University, Linköping SE-581 83, Sweden

ARTICLE INFO

Article history:
Received 7 December 2016
Received in revised form
21 December 2016
Accepted 23 December 2016
Available online 29 December 2016

ABSTRACT

The data presented in this paper are related to the research article entitled "Theoretical stability and materials synthesis of a chemically ordered MAX phase, Mo_2ScAlC_2, and its two-dimensional derivate Mo_2ScC" (Meshkian et al. 2017) [1]. This paper describes theoretical phase stability calculations of the MAX phase alloy $Mo_xSc_{3-x}AlC_2$ ($x=0, 1, 2, 3$), including chemical disorder and out-of-plane order of Mo and Sc along with related phonon dispersion and Bader charges, and Rietveld refinement of Mo_2ScAlC_2. The data is made publicly available to enable critical or extended analyzes.

Specifications Table

Subject area	Physics, Materials science
More specific subject area	Phase stability predictions,
Type of data	Tables, Figures, Text file
How data was acquired	Density functional theory calculations using VASP 5.3.3, phonon dispersion using Phonopy 1.9.1, and atom charges using Bader charge analysis version 0.95a.

* Corresponding author.
E-mail address: madah@ifm.liu.se (M. Dahlqvist).

http://dx.doi.org/10.1016/j.dib.2016.12.046

	θ-2θ X-ray diffraction (XRD) measurements were performed on the samples using a diffractometer (Rikagu Smartlab, Tokyo, Japan), with Cu-K_α radiation (40 kV and 44 mA). The scans were recorded between 3° and 120° with step size of 0.02° and a dwell time of 7 s.
Data format	Raw, Analyzed
Experimental factors	N/A
Experimental features	For synthesis of Mo_2ScAlC_2, elemental powders of Mo, Sc, Al and graphite were mixed in an agate mortar, put in an alumina crucible, and placed into a sintering furnace where it was heated up to 1700 °C and kept at that temperature for 30 min. Structural characterization was performed using X-ray diffraction (XRD), and for complementary structural and compositional analysis high-resolution scanning transmission electron microscopy (HRSTEM) measurement were carried out. See Ref. [1] for further information.
Data source location	Linköping, Sweden
Data accessibility	Data are available with this article.

Value of the data

- This data allows other researchers to calculate and predict the phase stability of new compounds within the quaternary Mo-Sc-Al-C system and related subsystem.
- The data presents refined/calculated structures that can be used as input for further theoretical evaluation of properties.
- The structural information can also be used for interpretation and phase identification of, e.g., attained experimental XRD, (S)TEM, and electron diffraction data.

1. Data

The dataset of this paper provides information for calculated phases within the quaternary Mo-Sc-Al-C system and data obtained from refinement of the XRD pattern. Table 1 provides calculated lattice

Table 1
Calculated lattice parameters, equilibrium total energy E_0 in eV per formula unit, formation enthalpy ΔH_{cp} in meV per atom, and identified equilibrium simplex for Mo_2ScAlC_2 and Sc_2MoAlC_2. For comparison the corresponding end members Mo_3AlC_2 and Sc_3AlC_2 are also included.

Phase	Order	a (Å)	c (Å)	E_0 (eV/fu)	ΔH_{cp} (meV/atom)	Equilibrium simplex
Mo_3AlC_2		3.0716	18.541	−54.830	+141	C, Mo_3Al
Mo_2ScAlC_2	A	3.0619	19.072	−52.431	–24	$(Mo_{2/3}Sc_{1/3})_2AlC$, MoC, $ScC_{0.875}$, Mo
Mo_2ScAlC_2	B	3.0774	19.252	−51.972	+53	$(Mo_{2/3}Sc_{1/3})_2AlC$, MoC, $ScC_{0.875}$, Mo
Mo_2ScAlC_2	C	3.1622	18.789	−51.601	+114	$(Mo_{2/3}Sc_{1/3})_2AlC$, MoC, $ScC_{0.875}$, Mo
Mo_2ScAlC_2	D	3.1771	18.865	−51.505	+130	$(Mo_{2/3}Sc_{1/3})_2AlC$, MoC, $ScC_{0.875}$, Mo
Mo_2ScAlC_2	E	3.1271	19.054	−51.348	+157	$(Mo_{2/3}Sc_{1/3})_2AlC$, MoC, $ScC_{0.875}$, Mo
Mo_2ScAlC_2	F	3.1221	19.109	−51.663	+104	$(Mo_{2/3}Sc_{1/3})_2AlC$, MoC, $ScC_{0.875}$, Mo
Mo_2ScAlC_2	disorder	3.1252	18.861	−51.767	+87	$(Mo_{2/3}Sc_{1/3})_2AlC$, MoC, $ScC_{0.875}$, Mo
Sc_2MoAlC_2	A	3.1798	19.819	−48.262	+28	$(Mo_{2/3}Sc_{1/3})_2AlC$, Sc_3AlC, Sc_3C_4
Sc_2MoAlC_2	B	3.1808	19.845	−48.071	+60	$(Mo_{2/3}Sc_{1/3})_2AlC$, Sc_3AlC, Sc_3C_4
Sc_2MoAlC_2	C	3.1886	19.696	−47.842	+98	$(Mo_{2/3}Sc_{1/3})_2AlC$, Sc_3AlC, Sc_3C_4
Sc_2MoAlC_2	D	3.1892	19.770	−47.864	+94	$(Mo_{2/3}Sc_{1/3})_2AlC$, Sc_3AlC, Sc_3C_4
Sc_2MoAlC_2	E	3.2279	19.802	−47.453	+162	$(Mo_{2/3}Sc_{1/3})_2AlC$, Sc_3AlC, Sc_3C_4
Sc_2MoAlC_2	F	3.1898	19.700	−47.779	+108	$(Mo_{2/3}Sc_{1/3})_2AlC$, Sc_3AlC, Sc_3C_4
Sc_2MoAlC_2	disorder	3.2251	19.335	−48.088	+57	$(Mo_{2/3}Sc_{1/3})_2AlC$, Sc_3AlC, Sc_3C_4
Sc_3AlC_2		3.3170	20.885	−43.406	+155	Sc_3AlC, Sc_3C_4, $ScAl_3C_3$

parameters, formation enthalpy, and equilibrium simplex for the chemically ordered nanolaminates Mo_2ScAlC_2 and Sc_2MoAlC_2 with different atomic stacking sequences (described in detail in Fig. 7(a) in Ref. [2]). Table 2 provides information for all considered competing phases within the quaternary system. Fig. 1 show calculated phonon spectra for Mo_2ScAlC_2 of order A and its corresponding end members Sc_3AlC_2 and Mo_3AlC_2. Fig. 2 depicts calculated Bader charges of atoms in $Mo_xSc_{3-x}AlC_2$ (x=0, 2, 3). Table 3 shows the data obtained from refinement of the XRD pattern, see Ref. [1]; Lattice vectors a, b and c for the majority phase Mo_2ScAlC_2 are 3.033, 3.033 and 18.775 Å, respectively.

Table 2
Structural information and calculated total energy for competing phases considered within the quaternary Mo-Sc-Al-C system.

Phase	Prototype structure	Pearson symbol	Space group	V (Å^3/uc)	a (Å)	b (Å)	c (Å)	E_0 (eV/fu)
Mo	W	*cI*2	*Im*-3*m* (229)	15.92	3.169			−10.850
Mo	Cu	*cF*4	*Fm*-3*m* (225)	16.15	4.012			−10.431
Mo	Mg	*hP*2	$P6_3/mmc$ (194)	32.57	2.774		4.887	−10.414
Sc	Mg	*hP*2	$P6_3/mmc$ (194)	49.25	3.321		5.157	−6.333
Sc	Sc	*hP*6	$P6_122$ (178)	148.75	3.242		16.342	−6.201
Sc	Np	*tP*4	P4/nmm (129)	100.35	5.367		3.484	−6.223
Al	Cu	*cF*4	*Fm*-3*m* (225)	66.00	4.041			−3.745
Al	Mg	*hP*2	$P6_3/mmc$ (194)	33.28	2.856		4.712	−3.712
Al	W	*cI*2	*Im*-3*m* (229)	16.93	3.235			−3.649
C	C (graphite)	*hP*4	$P6_3/mmc$ (194)	38.14	2.464		7.250	−9.225
Al_4C_3	Al_4C_3	*hR*21	*R*-3*m* h (166)	245.00	3.355		25.129	−43.340
$MoAl_{12}$	WAl_{12}	*cI*26	*Im*-3 (204)	436.23	7.584			−57.303
$MoAl_5$	$MoAl_5$	*hR*36	*R*-3*c* h (167)	558.49	4.952		26.296	−31.001
Mo_4Al_{17}	Mo_4Al_{17}	*mS*84	*C*121 (5)	1305.85	9.187	4.939	28.974	−112.563
Mo_3Al_8	Mo_3Al_8	*mS*22	*C*12/*m*1 (12)	334.46	9.235	3.653	10.091	−66.170
Mo_3Al	Cr_3Si	*cP*8	*Pm*-3*n* (223)	123.48	4.980			−37.228
Sc_2Al	Ni_2In	*hP*6	$P6_3/mmc$ (194)	128.50	4.902		6.176	−17.458
ScAl	CsCl	*cP*2	*Pm*-3*m* (221)	38.75	3.384			−10.973
ScAl	CrB	*oC*8	*Cmcm* (63)	81.00	3.338	11.101	4.371	−10.892
$ScAl_2$	$MgCu_2$	*cF*24	*Fd*-3*m* (227)	109.50	3.797			−15.277
$ScAl_3$	$AuCu_3$	*cP*4	*Pm*-3*m* (221)	69.25	4.107			−19.383
MoC	TiP	*hP*8	$P6_3/mmc$ (194)	84.84	3.016		10.768	−19.821
MoC	NaCl	*cF*8	*Fm*-3*m* (225)	21.06	4.383			−19.640
MoC	η-MoC	*hp*12	$P6_3/mmc$ (194)	126.16	3.074		15.401	−19.747
MoC	WC	*hp*2	*P*-6*m*2 (187)	21.00	2.928		2.829	−20.241
Mo_3C_2	Cr_3C_2	*oP*20	*Pnma* (62)	228.19	6.064	2.974	12.654	−50.938
Mo_2C	β''-Mo_2C	*hP*3	*P*-3*m*1 (164)	38.06	3.068		4.669	−31.064
Mo_3C	Fe_3C	*oP*16	*Pnma* (62)	215.87	5.540	7.559	5.159	−40.423
Sc_2C	Ti_2C	*cF*48	*Fd*-3*m* (227)	852.33	9.481			−23.266
Sc_4C_3	P_4Th_3	*cI*28	*I*-43*d* (220)	188.75	7.227			−56.419
$ScC_{0.875}$	NaCl	*cF*8	*Fm*-3*m* (225)	208.70	4.708			−14.923
ScC	NaCl	*cF*8	*Fm*-3*m* (225)	25.70	4.685			−15.840
Sc_3C_4	Sc_3C_4	*tP*70	*P*4/*mnc* (128)	851.50	7.515		15.076	−58.764
Mo_3AlC	$CaTiO_3$	*cP*5	*Pm*-3*m* (221)	71.70	4.154			−45.341
Mo_3Al_2C	Mo_3Al_2C	*cP*24	$P4_132$ (213)	327.20	6.891			−50.299
$Mo_3Al_2C_{0.9375}$	Mo_3Al_2C	*cP*24	$P4_132$ (213)	1303.30	6.881			−49.691
$Mo_3Al_2C_{0.875}$	Mo_3Al_2C	*cP*24	$P4_132$ (213)	648.29	6.869			−49.078
$Mo_3Al_2C_{0.875}$	Mo_3Al_2C	*cP*24	$P4_132$ (213)	1296.87	6.870			−49.069
$Mo_3Al_2C_{0.75}$	Mo_3Al_2C	*cP*24	$P4_132$ (213)	321.10	6.848			−47.844
Mo_2AlC	Cr_2AlC	*hP*8	$P6_3/mmc$ (194)	107.46	3.031		13.505	−35.292
Mo_3AlC_2	Ti_3SiC_2	*hP*12	$P6_3/mmc$ (194)	151.49	3.072		18.541	−54.830
Mo_4AlC_3	Ti_4AlN_3	*hP*16	$P6_3/mmc$ (194)	196.50	3.117		23.358	−74.552
$(Mo_{2/3}Sc_{1/3})_2AlC$	$(Mo_{2/3}Sc_{1/3})_2AlC$	mS48	*C*2/*c* (15)	689.78	9.367	5.427	13.961	−33.308
$ScAl_3C_3$	$ScAl_3C_3$	*hP*14	$P6_3/mmc$ (194)	164.34	3.362		16.789	−47.703
Sc_3AlC	$CaTiO_3$	*cP*5	*Pm*-3*m* (221)	84.90	4.395			−35.023
Sc_2AlC	Cr_2AlC	*hP*8	$P6_3/mmc$ (194)	141.75	3.296		15.065	−27.385
Sc_3AlC_2	Ti_3SiC_2	*hP*12	$P6_3/mmc$ (194)	199.00	3.317		20.885	−43.406
Sc_4AlC_3	Ti_4AlN_3	*hP*16	$P6_3/mmc$ (194)	248.50	3.296		26.414	−59.294

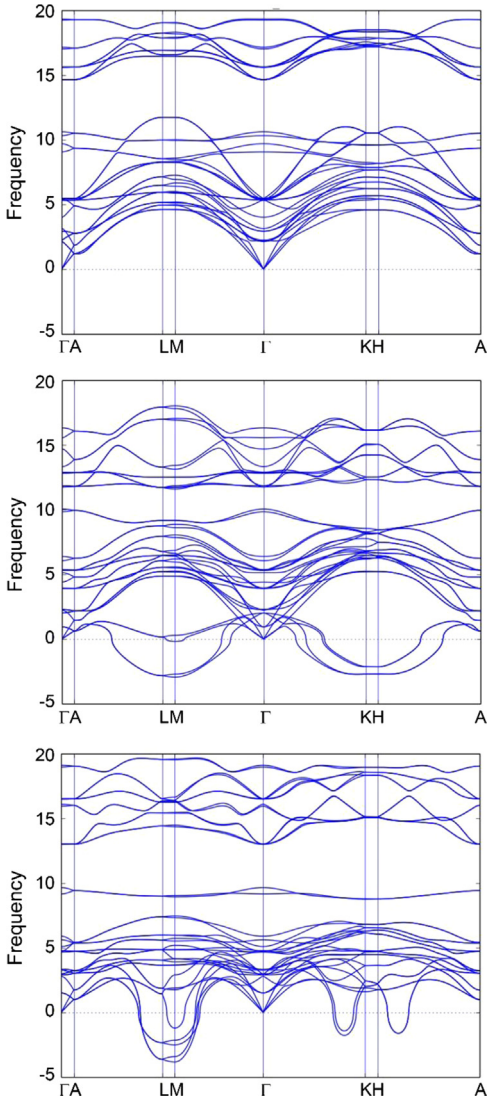

Fig. 1. Calculated phonon dispersion for (a) Mo_2ScAlC_2, (b) Sc_3AlC_2, and (c) Mo_3AlC_2.

2. Experimental design, materials and methods

First-principles calculations were performed by means of density functional theory (DFT) and the projector augmented wave method [3,4] as implemented within the Vienna ab-initio simulation package (VASP) 5.3.3 [5–7]. We adopted the non-spin polarized generalized gradient approximation (GGA) as parameterized by Perdew–Burke–Ernzerhof (PBE) [8] for treating electron exchange and correlation effects. A plane-wave energy cut-off of 400 eV was used and for sampling of the Brillouin zone we used the Monkhorst–Pack scheme [9]. The calculated total energy of all phases is converged to within 0.5 meV/atom with respect to k-point sampling and structurally optimized in terms of unit-cell volumes, c/a ratios (when necessary), and internal parameters to minimize the total energy.

Chemically disordered of Sc and Mo in $Mo_xSc_{3-x}AlC_2$ have been modelled using the special quasi-random structure (SQS) method [10,11] on supercells of $4 \times 4 \times 1$ M_3AX_2 unit cells, with a total of 96

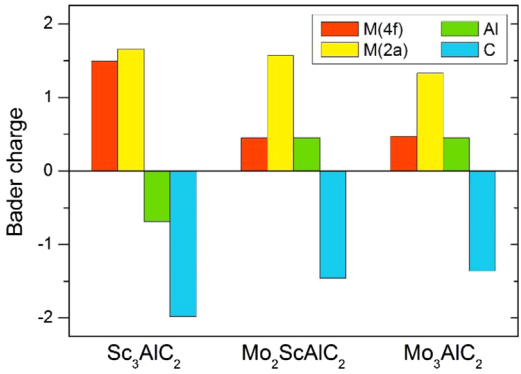

Fig. 2. Calculated charge for atoms in Sc_3AlC_2, Mo_2ScAlC_2, and Mo_3AlC_2 using Bader analysis.

Table 3
Rietveld refinement of Mo_2ScAlC_2. The identified phases and their respective weight percentages according to the Rietveld refinement of the XRD pattern are: 1. Mo_2ScAlC_2 (73.9(0) wt.%), Mo_2C (14.1(8) wt.%), $A1_2O_3$ (7.4(0) wt.%), Mo_3Al_2C (3.5(0) wt.%) and, Mo_3Al (1.0(2) wt.%), the total χ^2 is 10.50.

Space group	*P6₃/mmc* (#194)
a (Å)	3.0334(8)
b (Å)	3.0334(8)
c (Å)	18.7750(0)
α	90.000
β	90.000
γ	120.000
Mo	4f (0.3333(3) 0.6666(7) 0.1363(2))
	Occupancy of Mo=4.00(0) and Sc=0.00(0)
Sc	2a (0.0000 0.0000 0.0000)
	Occupancy of Sc=1.83(4) and Mo=0.16(6)
Al	2b (0.0000 0.0000 0.2500) Occupancy of Al=2.00
C	4f (0.6666(7) 0.3333(3) 0.06825(5)) Occupancy of C=4.00

M-sites, respectively. Convergence tests with respect to total energy show that these sizes are appropriate to use, based on an energy of the $4 \times 4 \times 1$ unit cells being within 2 meV/atom compared to larger supercells.

Evaluation of phase stability was performed by identifying the set of most competing phases at a given composition, i.e. equilibrium simplex, using a linear optimization procedure [11,12] including all competing phases in the system. A phase is considered thermodynamically stable when its energy is lower than the set of most competing phases, and when there is no imaginary frequencies in phonon spectra, i.e. an indicated dynamic stability. The approach has been proven successful to confirm already experimentally known MAX phases as well as to predict the existence of new ones [2,13,14].

Dynamical stability of the chemically ordered $Mo_xSc_{3-x}AlC_2$ ($x=0, 2, 3$) structures was evaluated by phonon calculations of $4 \times 4 \times 1$ supercells using density functional perturbation theory and as implemented in the PHONOPY code, version 1.9.1 [15,16]. Calculated charges were obtained using Bader charge analysis, version 0.95a [17].

The synthesis of Mo2ScAlC2 were carried out by mixing elemental powders of Mo, Sc, Al and graphite in an agate mortar, put in an alumina crucible, and placed into a sintering furnace where it was heated up to 1700 °C and kept at that temperature for 30 min.

θ-2θ X-ray diffraction (XRD) measurements were performed on the samples using a diffractometer (Rikagu Smartlab, Tokyo, Japan), with Cu-K_α radiation (40 kV and 44 mA). The scans were recorded between 3° and 120° with step size of 0.02° and a dwell time of 7 s. XRD pattern was analyzed by Rietveld refinement using FULLPROF code [18], where 5 backgrounds parameters, scale factors, *X* and *Y* profile parameters, lattice parameters, atomic positions, the overall B-factor and the occupancies for the main as well as the impurity phases were fitted.

Funding sources

J. R. acknowledges funding from the Swedish Research Council (VR) under Grant no. 621-2012-4425 and 642-2013-8020, from the Knut and Alice Wallenberg (KAW) Foundation, and from the Swedish Foundation for Strategic Research (SSF) through the synergy grant FUNCASE. All calculations were carried out using supercomputer resources provided by the Swedish National Infrastructure for Computing (SNIC) at the National Supercomputer Centre (NSC), the High Performance Computing Center North (HPC2N), and the PDC Center for High Performance Computing.

Transparency document. Supplementary material

Transparency document associated with this paper can be found in the online version at http://dx.doi.org/10.1016/j.dib.2016.12.046.

Appendix A. Supplementary material

Supplementary material associated with this paper can be found in the online version at http://dx.doi.org/10.1016/j.dib.2016.12.046.

References

[1] R. Meshkian, Q. Tao, M. Dahlqvist, J. Lu, L. Hultman, J. Rosen, Theoretical stability and materials synthesis of a chemically ordered MAX phase, Mo_2ScAlC_2, and its two-dimensional derivate Mo_2ScC_2 MXene, Acta Mater. (2016).
[2] B. Anasori, M. Dahlqvist, J. Halim, E.J. Moon, J. Lu, B.C. Hosler, E.N. Caspi, S.J. May, L. Hultman, P. Eklund, J. Rosén, M. W. Barsoum, Experimental and theoretical characterization of ordered MAX phases Mo_2TiAlC_2 and $Mo_2Ti_2AlC_3$, J. Appl. Phys. 118 (2015) 094304.
[3] P.E. Blöchl, Projector augmented-wave method, Phys. Rev. B 50 (1994) 17953–17979.
[4] G. Kresse, D. Joubert, From ultrasoft pseudopotentials to the projector augmented-wave method, Phys. Rev. B 59 (1999) 1758–1775.
[5] G. Kresse, J. Hafner, Ab initio molecular dynamics for liquid metals, Phys. Rev. B 47 (1993) 558–561.
[6] G. Kresse, J. Furthmüller, Efficiency of ab-initio total energy calculations for metals and semiconductors using a plane-wave basis set, Comput. Mater. Sci. 6 (1996) 15–50.
[7] G. Kresse, J. Furthmüller, Efficient iterative schemes for ab initio total-energy calculations using a plane-wave basis set, Phys. Rev. B 54 (1996) 11169–11186.
[8] J.P. Perdew, K. Burke, M. Ernzerhof, Generalized gradient approximation made simple, Phys. Rev. Lett. 77 (1996) 3865–3868.
[9] H.J. Monkhorst, J.D. Pack, Special points for Brillouin-zone integrations, Phys. Rev. B 13 (1976) 5188–5192.
[10] A. Zunger, S.H. Wei, L.G. Ferreira, J.E. Bernard, Special quasirandom structures, Phys. Rev. Lett. 65 (1990) 353–356.
[11] M. Dahlqvist, B. Alling, I.A. Abrikosov, J. Rosén, Phase stability of Ti_2AlC upon oxygen incorporation: a first-principles investigation, Phys. Rev. B 81 (2010) 024111–024118.
[12] M. Dahlqvist, B. Alling, J. Rosén, Stability trends of MAX phases from first principles, Phys. Rev. B 81 (2010) 220102.
[13] P. Eklund, M. Dahlqvist, O. Tengstrand, L. Hultman, J. Lu, N. Nedfors, U. Jansson, J. Rosén, Discovery of the ternary nanolaminated compound Nb_2GeC by a systematic theoretical-experimental approach, Phys. Rev. Lett. 109 (2012) 035502.
[14] A.S. Ingason, A. Mockute, M. Dahlqvist, F. Magnus, S. Olafsson, U.B. Arnalds, B. Alling, I.A. Abrikosov, B. Hjörvarsson, P.O. Å. Persson, J. Rosen, Magnetic self-organized atomic laminate from first principles and thin film synthesis, Phys. Rev. Lett. 110 (2013) 195502.

[15] A. Togo, F. Oba, I. Tanaka, First-principles calculations of the ferroelastic transition between rutile-type and $CaCl_2$-type SiO_2 at high pressures, Phys. Rev. B 78 (2008) 134106.
[16] A. Togo, I. Tanaka, First principles phonon calculations in materials science, Scr. Mater. 108 (2015) 1–5.
[17] G. Henkelman, A. Arnaldsson, H. Jónsson, A fast and robust algorithm for Bader decomposition of charge density, Comput. Mater. Sci. 36 (2006) 354–360.
[18] H.M. Rietveld, A profile refinement method for nuclear and magnetic structures, J. Appl. Crystallogr. 2 (1969) 65–71.